J. Fluid Mech. (1989), *vol.* 207, *pp.* 475–487
Printed in Great Britain

A numerical and experimental investigation of a new solution in the Taylor vortex problem

By D. K. ANSON[1]†, T. MULLIN[2] AND K. A. CLIFFE[3]

[1] Mathematical Institute, Oxford University, Oxford OX1 3LB, UK

[2] Clarendon Laboratory, Parks Road, Oxford OX1 3PU, UK

[3] Theoretical Physics Division, UKAEA, Harwell Laboratory, Oxon OX11 0RA, UK.

(Received 10 November 1988)

We present the results of a numerical and experimental study of the five-cell flow in the Taylor vortex problem. There is evidence for a new five-cell solution which is different in nature to the previously recorded solution. We find that there is an exchange in stability between the two solutions which we explain in terms of bifurcation theory. Streamline plots of the numerical results are compared with photographs of the observed flow. The agreement between the calculations and experiments is good. We use the Schaeffer homotopy to study the new solution in the periodic model. The results show that the new solution is not connected in any continuous manner to the trivial Couette flow solution.

1. Introduction

In recent years, several studies have reported evidence of novel cellular states in the Taylor vortex problem. In these flows the direction of spiralling of at least one of the end cells leads to outward motion along the fixed endwall. Examples of such states were first observed by Benjamin in 1978. Since then, there has been significant theoretical, numerical and experimental work by, amongst others, Benjamin & Mullin (1981), Cliffe & Mullin (1985) and Bolstad & Keller (1987).

In these experiments the inner cylinder rotates whilst the outer cylinder and both ends are held fixed. Intuition suggests that the flow produced in this way should be directed inward at the ends. Similarly, one might suppose that the number of cells should be even, owing to the imposed symmetry of the boundary conditions. Indeed such flows are well known in the Taylor problem and are termed normal modes. The primary flow is defined to be that developed by a gradual increase in the Reynolds number from small values and always consists of one of these normal modes.

However, the modes which interest us in the present study do not fall into this category. They form a class of flows which had apparently gone unnoticed in over fifty years of research into the problem until Benjamin's observations in 1978. Therefore, he called them anomalous modes. Such modes can be considered to originate from the periodic model and the labelling of the cellular states is chosen to be consistent with this observation. Further support for this reasoning is given by the major cellular motion observed experimentally, which gives outward flow along one or both ends, notwithstanding the small weak circulation in the corners.

It is well known that all secondary modes, with one exception, are disconnected from the primary flow, and cannot survive below a critical value of the Reynolds

† Present address: ICI Corporate Management Services, Brunner Business Centre, Brunner House, PO Box 7, Winnington, Northwich, Cheshire CW8 4DJ, UK.

number. In the periodic model, however, mathematical analysis and numerical results have shown that these modes all bifurcate from the trivial solution. In 1981, Benjamin & Mullin suggested a bifurcation diagram representing a mechanism for producing disconnected modes, starting from the periodic model. The construction of the diagram is based on the work of Benjamin (1978*a*, *b*) and Schaeffer (1980). Schaeffer introduced a homotopy between the abstract model, with periodic boundary conditions, and the realistic model, with no-slip conditions, with the homotopy parameter τ taking the value 0 in the former and 1 in the latter.

The simplest example of an anomalous mode has one cell. In the state diagram at $\tau = 0$ this case is represented by a symmetric bifurcation from the trivial solution. Such a bifurcation necessarily breaks the midplane symmetry of the primary flow. Benjamin & Mullin (1981) speculated that the bifurcation persists to $\tau = 1$ for a sufficiently small value of the aspect ratio, Γ. As Γ is increased the single-cell modes then become disconnected.

Benjamin & Mullin (1981) also presented experimental evidence to support these conjectures, which are given further credence by the numerical results of Cliffe (1983) and the experimental work of Pfister *et al.* (1988). It is also suggested that, in the case of odd-cell flows with $N \geqslant 3$ the sequence of qualitative changes is the same as for single-cell flows, but that the disconnection process takes place at values of τ less than 1.

Indeed, Cliffe & Mullin (1985) produced numerical and experimental evidence to support these speculations. In an independent investigation, Bolstad & Keller (1987) used the same model to account for the disconnected five-cell modes and computed the five-cell solution by a numerical implementation of the Schaeffer homotopy. The results again confirmed the theory of Benjamin & Mullin (1981).

Comparisons of numerical and experimental results based on the use of Schaeffer's homotopy, reported in the above studies, give convincing qualitative and quantitative agreement. We consider that the use of the homotopy is justified and use the same approach in the present study.

Bolstad & Keller (1987) computed the lower stability boundary for the five-cell mode by numerical methods. The diagram of their results has a cusp in the lower left part of the curve at $\tau = 1$. Cliffe & Mullin (1985) have also noticed the existence of such a feature, which has certain implications in bifurcation theory.

In the present study, we again compute the five-cell solution stability curve and make comparisons with new experimental observations. We find numerical and experimental evidence for a new five-cell flow which exchanges stability with the previously recorded five-cell flow at a critical value of Γ. We shall refer to the previously recorded five-cell flow as the 'old' five-cell solution. We find that the mechanism for the stability exchange involves a transcritical bifurcation and a hysteresis point. However, this feature alone does not account for the changes in stability of the solutions. We must also take into account a path of Hopf points bifurcating to unstable time-periodic flow.

A further interesting feature is that the new flow is found to exist as a disconnected mode in the periodic model. That is to say, that while the old five-cell flow arises at a symmetry-breaking bifurcation from the trivial Couette flow solution, the new flow simply appears from a limit point at a critical value of the Reynolds number.

The experimental procedure used in this study is the same as that described in §4 of Cliffe & Mullin (1985): we do not repeat the description here.

In §2 we describe the numerical methods and bifurcation techniques, in §3 we present the results and finally in §4 we draw some conclusions.

2. Numerical methods

We now proceed to outline the numerical methods used in the present study and also consider several theoretical points which are important in the interpretation of the numerical results. Let us first recall the methods of Cliffe & Mullin (1985) for approximating the steady-state Navier–Stokes equations.

Keller arclength continuation methods are applied to a finite set of equations of the form

$$\boldsymbol{f}(\boldsymbol{x}, R, \Gamma, \eta, \tau) = \boldsymbol{0}, \quad \boldsymbol{f}: \boldsymbol{X} \times \mathbb{R}^4 \rightarrow \boldsymbol{X}, \tag{2.1}$$

obtained from a finite-element discretization of the Navier–Stokes equations over the rectangular cross-section of an annular fluid-filled region. This region, of width d and length l, is bounded by an inner cylinder of radius r_1 rotating with angular speed Ω and a stationary outer cylinder of radius r_2.

In these equations $\boldsymbol{x}$ is the solution vector, consisting of all the velocity and pressure degrees of freedom and $\boldsymbol{X}$ is the high-dimensional space representing all the degrees of freedom allowed for $\boldsymbol{x}$. We define the Reynolds number to be $R = \Omega r_1 d/\nu$, where ν is the kinematic viscosity, the aspect ratio to be $\Gamma = l/d$ and the radius ratio to be $\eta = r_2/r_1$. In the present study η is fixed at a value of 0.6.

We apply the equations (2.1) over the region

$$D = \{(r, z): r_1 < r < r_2, -\tfrac{1}{2}l < z < \tfrac{1}{2}l\}. \tag{2.2}$$

Boundary conditions applied in the derivation of (2.1) require that u_r and u_z vanish on both cylindrical surfaces and that $u_\phi = 0$ on the outer cylinder and $u_\phi = 1$ on the inner cylinder. We use the boundary conditions proposed by Schaeffer (1980) on the ends of the annulus,

$$\left.\begin{aligned} u_z &= 0, \\ (1-\tau)\frac{\partial u_r}{\partial z} \pm \tau u_r &= 0, \\ (1-\tau)\frac{\partial u_\phi}{\partial z} \pm \tau(u_\phi - F(r)) &= 0, \end{aligned}\right\} \tag{2.3}$$

for $z = \pm\frac{1}{2}l$ and $r_1 \leqslant r \leqslant r_2$. Here $F(r)$ is a smooth function satisfying $F(r_1) = 1$ and $F(r) = 0$ for $r \geqslant r_1 + \epsilon$, with $0 < \epsilon \ll r_2 - r_1$ (Benjamin & Mullin 1981, p. 232).

We turn briefly to a discussion of the bifurcation theory employed in the present study. We are concerned with the bifurcations to four- and five-cell flow, from the trivial solution in the periodic model. The bifurcation to five-cell flow, labelled P_1 in figure 1(*a*) and figure 2(*a*) breaks the midplane symmetry of the solution and is known as a symmetry-breaking bifurcation. The bifurcation to four-cell flow, labelled P_2, in figure 1(*a*) and figure 2(*a*) does not break the midplane symmetry, although the bifurcating branches do lie in a different subspace to the trivial solution. It is therefore known as a subspace-breaking bifurcation. The main difference between the two bifurcations in the present context is that, when τ is increased from zero, the symmetry-breaking bifurcation persists, whilst the subspace-breaking bifurcation decouples to give a limit point. As we see in figures 1 and 2, there are two secondary bifurcations, S_1 and S_2, which lie either on the five-cell mode where they are subspace-breaking or on the four-cell mode where they are symmetry-breaking. The ordering of the bifurcations depends on Γ and changes at the multiple bifurcation point, Γ_m.

We now consider the implications of applying the homotopy to transform from the periodic model to the realistic model. As we increase τ from zero, the bifurcation to

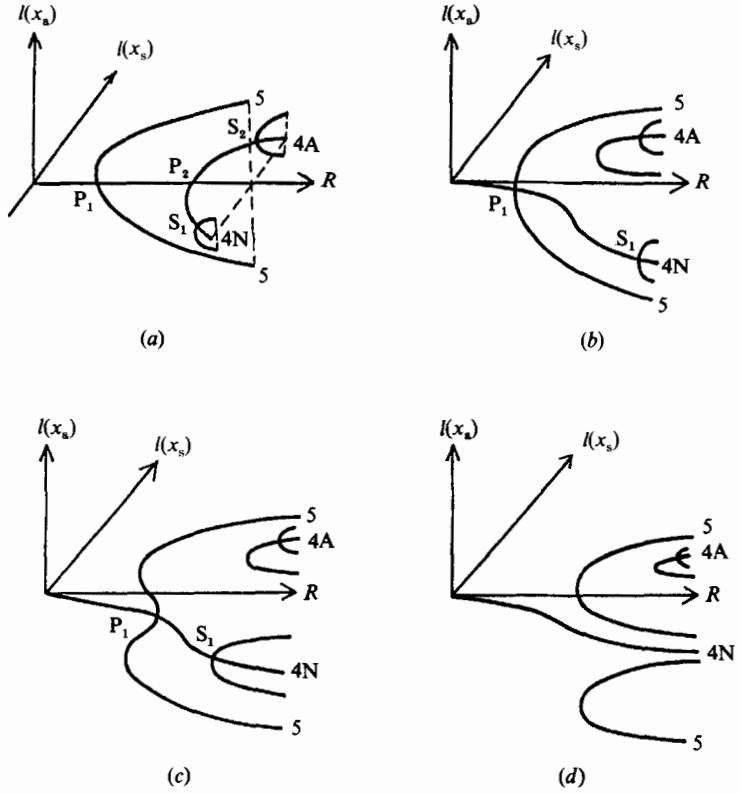

FIGURE 1. State diagrams representing the decoupling of the five-cell anomalous modes, as τ is increased from 0 (*a*) to 1 (*d*), for $\Gamma > \Gamma_m$ (Γ_m is the value of Γ at which the four- and five-cell bifurcations change priority at $\tau = 0$).

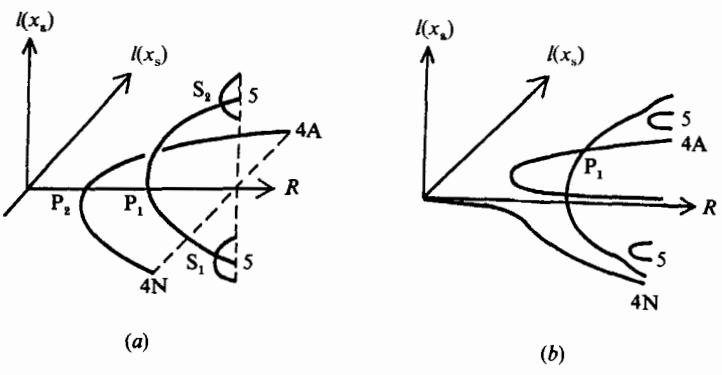

FIGURE 2. State diagrams representing the decoupling of the five-cell anomalous modes, as τ is increased from 0 (*a*) to 1 (*b*), for $\Gamma < \Gamma_m$.

five-cell flow persists, since it is symmetry breaking. It does not, however, persist to $\tau = 1$, and as a result the five-cell modes are disconnected at $\tau = 1$. The disconnected modes are generated in one of two ways depending on whether $\Gamma > \Gamma_m$ or $\Gamma < \Gamma_m$, as we see in the schematic representation of figure 1 and figure 2.

In the present study we fixed Γ at 4.7, a value greater than Γ_m, and the bifurcation process is represented by figure 1 (*a–d*). We compute the path of symmetry-breaking

bifurcations using an extended system of equations formulated by Werner & Spence (1984). As τ is increased, the supercritical bifurcation, P_1, first becomes subcritical then coalesces with the supercritical bifurcation, S_1, to produce the disconnected five-cell modes. These two events occur at points of higher-order singularity on the solution surface and are known as quartic points and coalescence points respectively (Cliffe & Spence 1984). They may be considered to be singularities on the path of symmetry-breaking bifurcations.

Before we can compute the path of symmetry-breaking bifurcations we require an approximation of the solution near P_1. We obtain this approximation by applying a continuation procedure along the trivial solution at $\tau = 0$. The singular point is detected by a change in sign of the determinant of the Jacobian matrix. We locate the singular point exactly by use of the extended system and compute the path of symmetry-breaking bifurcations as τ is increased from zero. We proceed until both a quartic point and a coalescence point have been detected, using a method given in Cliffe & Spence (1984).

We now fix τ at a value greater than that of the quartic point and continue along a branch of the subcritical bifurcation. The techniques used for switching branches at a bifurcation point can be found in Keller (1977). We proceed until a limit point is detected, again by monitoring the sign of the determinant of the Jacobian matrix. A limit point may be characterized as an isolated solution of an extended system of equations formulated by Moore & Spence (1980). We compute the locus of limit points by increasing τ to 1, noting that as τ is increased the five-cell modes become disconnected at the coalescence point.

The path of limit points, at $\tau = 1$, represents the lower stability boundary of the five-cell flow in the experiments. We compute the path of these points in the same way as before, using Γ as the continuation parameter, with τ fixed at 1. (This is the value of τ used for all comparisons between calculation and experiment.)

On paths of limit points we may detect two types of higher-order singularity, namely a hysteresis point and a transcritical bifurcation point. Such points are located by use of extended systems formulated by Jepson & Spence (1985). We may also check for bifurcation to time-dependent flow. Under certain conditions a path of Hopf bifurcation points can arise from the fold curve. The start of this path coincides with a singularity on the fold curve which can be detected by monitoring the defining conditions. Extended systems for this singularity, known as the Takens–Bogdanov point (Guckenheimer & Holmes 1986), and for Hopf bifurcation points have been devised by Jepson, Spence & Cliffe (1988) and Griewank & Reddien (1983), respectively.

Recall from the introduction that we have found evidence for a new five-cell solution. This solution is located numerically by applying continuation in both Γ and R. We have been able to compute the path of limit points of the new solution, at $\tau = 1$, as well as tracing the solution back to $\tau = 0$, by following the path of limit points. The aim of the second computation is to investigate the new solution in relation to the existing bifurcation model for the periodic approximation.

3. Results

Figure 3 represents a comparison between the numerically calculated curves and the new experimental results, for a radius ratio of 0.6. The experimental results correspond to parameter values (Γ, R) at which a stable, steady five-cell solution loses stability. The numerically calculated curve 5_0 represents the path of limit points of

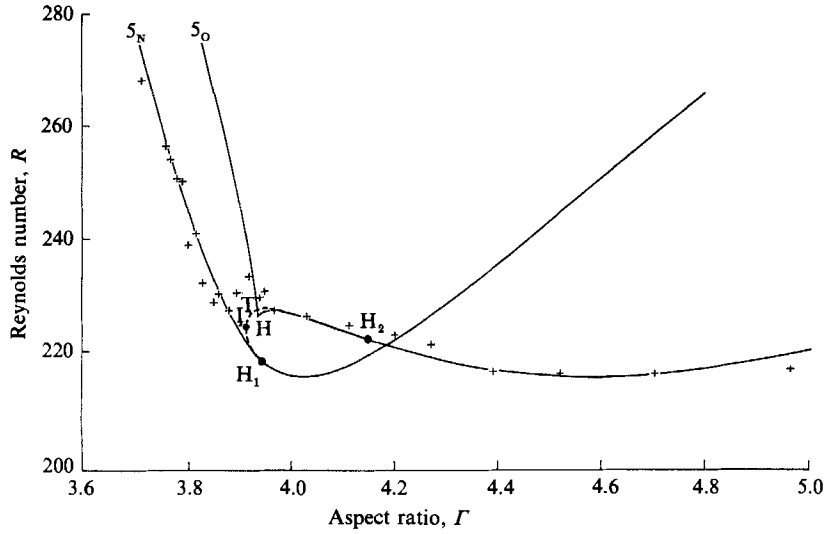

FIGURE 3. Critical loci for the five-cell anomalous modes with radius ratio 0.6; +, experiment; ——, numerically calculated fold curve of 5_O, the old solution, 5_N the new solution; – – –, numerically calculated path of Hopf bifurcation points (NB. this connects H_1 and H_2 but lies very close to the lower limit of stability of the 5_O solution over part of its length).

the old five-cell solution while 5_N represents the path of limit points of the new five-cell solution. The curve joining the Takens–Bogdanov points, H_1 and H_2, is a path of Hopf bifurcation points. The point I represents the point at which this path is tangential to the R-axis. There are singularities on the fold curve at T, a transcritical bifurcation point, and at H, a hysteresis point.

There are three distinct regions of the (Γ, R)-plane determined by aspect ratio. In the first region, given by $\Gamma < \Gamma_I$, a stable five-cell flow exists above the curve 5_N. In the region $\Gamma_I < \Gamma < \Gamma_{H2}$ we have a stable five-cell flow above the curve joining H_2 and I and in the small region between the curve joining H_1 and I and the locus of 5_N. Finally for $\Gamma > \Gamma_{H2}$, there is a stable five-cell flow above the curve 5_O.

In the region around I it was very difficult to obtain repeatable experimental results and thus the fine detail of the numerical work could not be resolved experimentally. In each of these regions there is no experimental evidence for a stable five-cell solution below the specified curve. These results indicate that the observable five-cell state for $\Gamma < \Gamma_I$ is different to that for $\Gamma > \Gamma_T$. In particular we should expect the solution for $\Gamma < \Gamma_I$ to be the new five-cell state and the solution for $\Gamma > \Gamma_T$ to be the old five-cell state. For the intermediate range of Γ it is not immediately obvious which state we should expect. In figures 4 and 5 there is a comparison between cross-sectional photographs and streamline plots for a value of Γ less than Γ_I (figure 4) and a value greater than Γ_T (figure 5). In figure 4(*a*), the streamline plot obtained numerically from the new five-cell solution at $\Gamma = 3.785$, $R = 253$, compares favourably with the photograph of the experimentally observed flow at the same parameter values (figure 4*b*). In figure 5(*a*), the streamline plot was obtained from the old five-cell solution at $\Gamma = 4.595$, $R = 217.8$ and again there is a good comparison with the photograph of the experimentally observed flow at these parameter values (figure 5*b*). The main difference between the two five-cell states is the much smaller size of the second and third cells from the top, in figures 4 and 5, in the new state than in the old state.

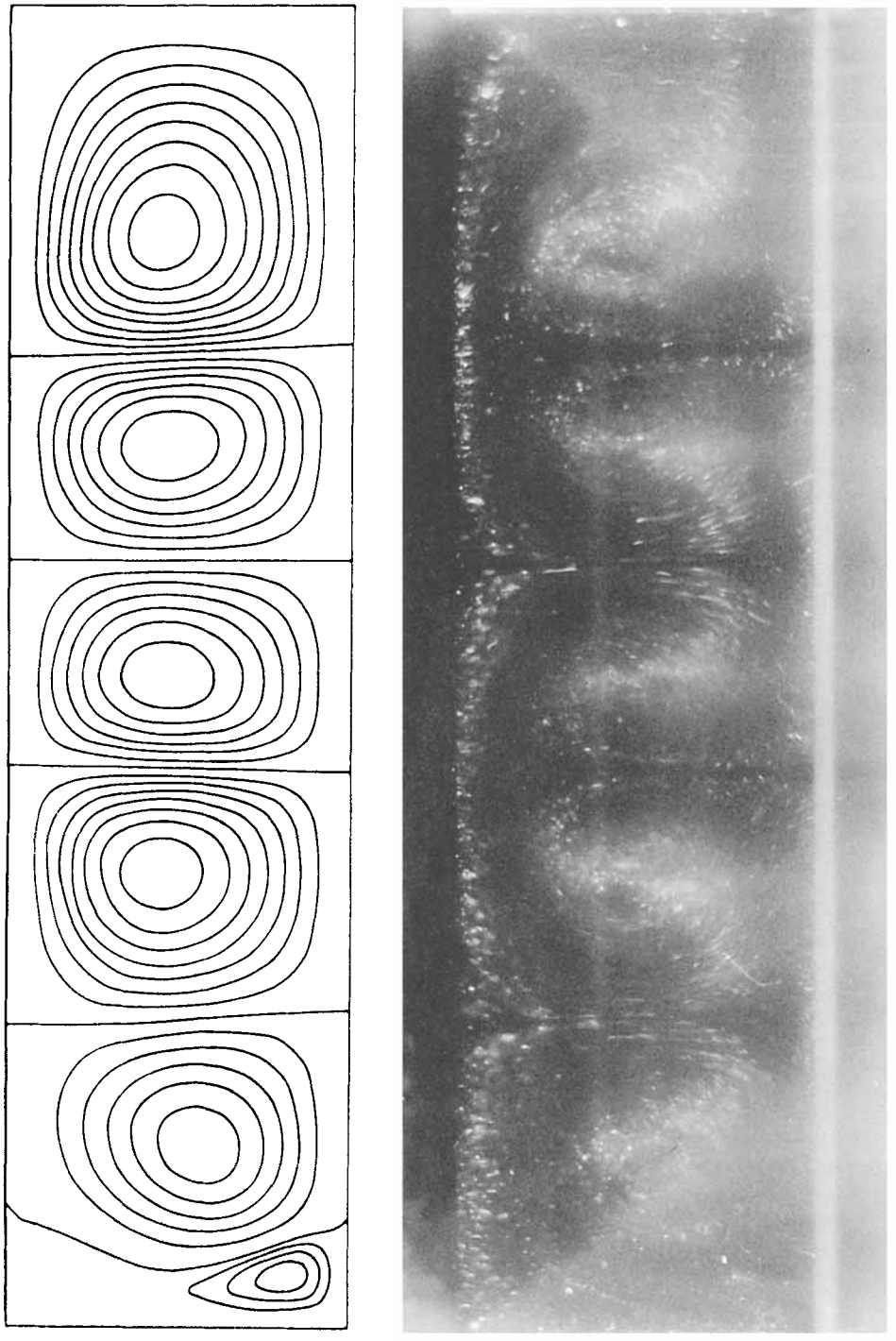

(*a*) (*b*)

FIGURE 4. Streamline plot of numerical solution (*a*) and photograph (*b*) for $\eta = 0.6$, $\Gamma = 3.785$, $R = 253$, of the five-cell flow. Contours of the stream function are plotted at intervals of 0.01 except for the small vortex in the corner where the interval is 0.0025.

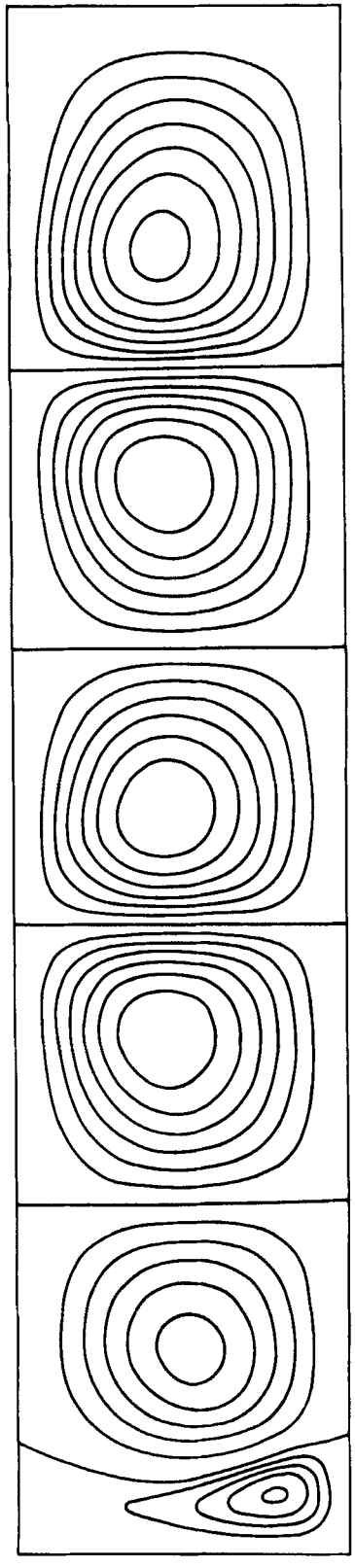

(a)

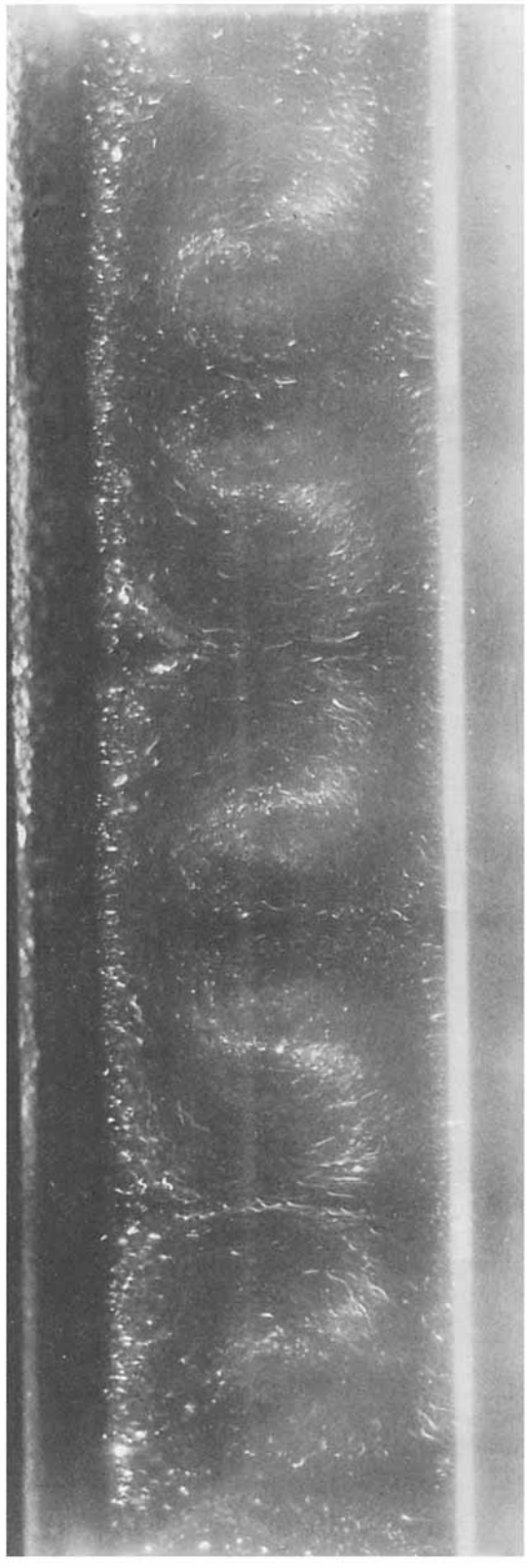

(b)

FIGURE 5(a, b). For caption see facing page.

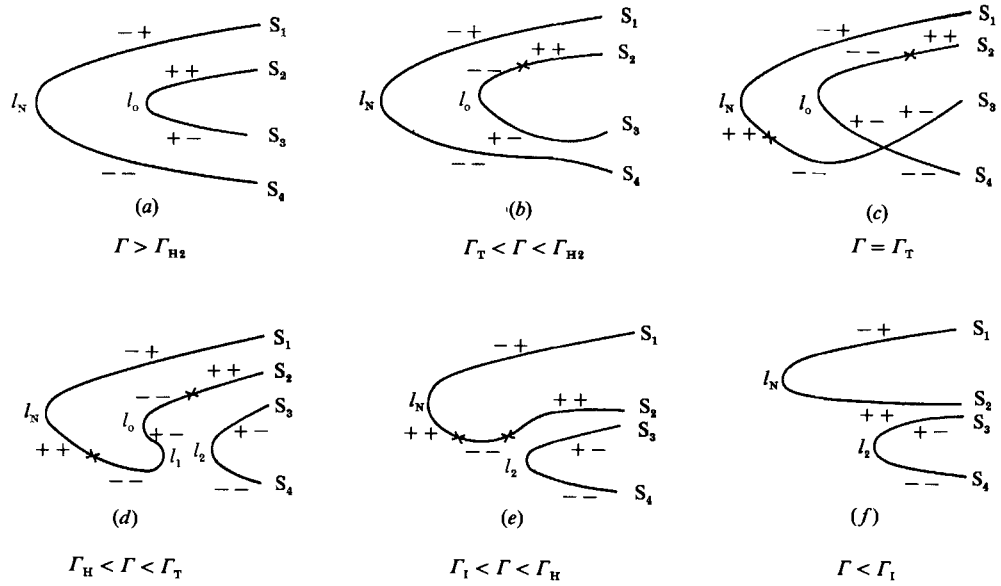

FIGURE 6. Changes in the bifurcation diagram for the old five-cell mode and the new five-cell mode, at $\tau = 1$, as Γ is decreased from about 4.16 to 3.88. The stabilities are indicated by $++$, stable; $--$, $+-$ and $-+$, unstable. Hopf bifurcation points are marked $\times$.

We now give an explanation of the above results with reference to the schematic diagrams in figure 6. The eigenvalues are indicated by $+$ and $-$ signs, where $++$ means no negative eigenvalues and $--$ indicates a pair of negative eigenvalues. Only $++$ gives rise to a stable solution. The sequence 6(*a*) to 6(*f*) is arranged in order of decreasing values of Γ, with the critical values referring to the singularities of figure 3.

In figure 6(*a*), $\Gamma > \Gamma_{H2}$, the only stable state lies on the old solution. The critical Reynolds number is determined by the limit point ℓ_O, which lies on the fold curve 5_O. At $\Gamma = \Gamma_{H2}$, a Hopf bifurcation point appears on the stable branch of the old solution, destabilizing part of the solution as shown in figure 6(*b*). The solution for $\Gamma_{H_2} > \Gamma > \Gamma_T$ is given in figure 5(*b*). At $\Gamma = \Gamma_{H1}$ a second Hopf bifurcation appears, this time on the doubly unstable branch of the new solution, thus stabilizing it as shown in figures 6(*c*), 6(*d*) and 6(*e*). In theory, therefore, we might expect a stable flow to exist between the limit point l_N and the Hopf point. In practice the range of R is so small that we do not observe it experimentally, instead the lower stability boundary of the stable flow is marked by the Hopf point on the old solution. At $\Gamma = \Gamma_T$ there is a transcritical bifurcation which leads to the appearance of two new limit points, l_1 and l_2, (see figure 6*c* and 6*d*) and a hysteresis loop. At $\Gamma = \Gamma_H$, the hysteresis loop straightens out and we are left with the solution in figure 6(*e*). The old solution is now completely unstable while the stable branch of the new solution is destabilized over a small range of Reynolds number by the two Hopf bifurcation points. At $\Gamma = \Gamma_I$ these two points coalesce and the new solution has a completely

FIGURE 5. Streamline plot of numerical solution (*a*) and photograph (*b*) for $\eta = 0.6$, $\Gamma = 4.595$, $R = 217.8$ of the five-cell flow. Contours of the stream function are plotted at intervals of 0.01 except for the small vortex in the corner where the interval is 0.0025.

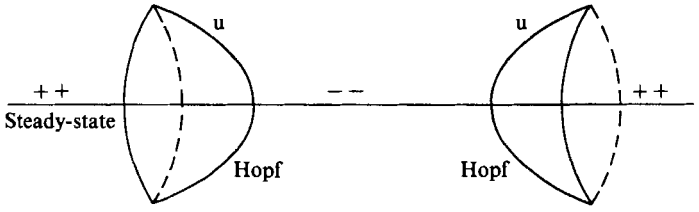

FIGURE 7. Conjectured representation of the Hopf bifurcation points, and resulting periodic orbits, on the new five-cell solution for $\Gamma_1 < \Gamma < \Gamma_H$, with the stabilities indicated on the steady-state solution by ++, stable and --, unstable; and on the periodic orbits by u, unstable.

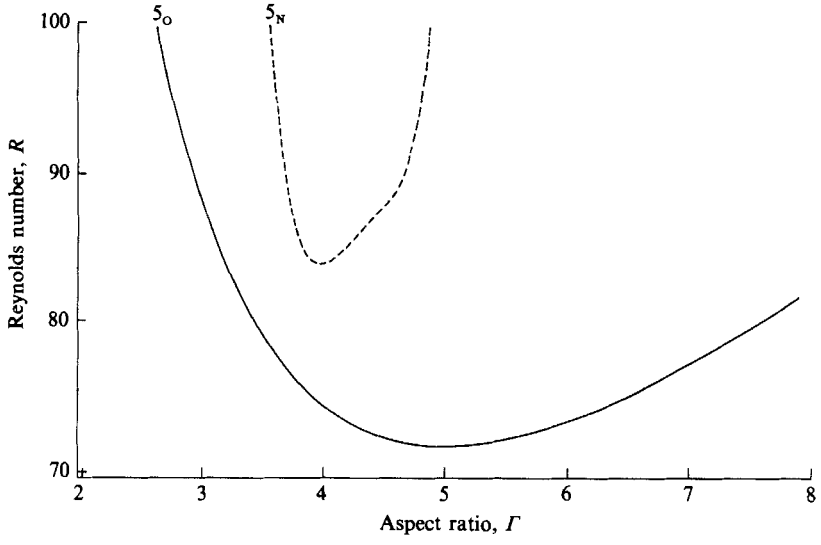

FIGURE 8. Numerically calculated path of symmetry-breaking bifurcation points for the old five-cell mode (——) numerically calculated fold curve for the new five-cell mode (– – –), with radius ratio 0.6 and $\tau = 0$.

stable branch. The lower stability boundary is marked by the limit point ℓ_N which lies on the fold curve 5_N. We have not determined numerically the stability of the periodic orbits resulting from the two Hopf bifurcation points, but since no stable oscillatory flows were observed we assume that the orbits are unstable. This assumption leads to the conjectured bifurcation diagram shown in figure 7.

It is now left to discuss the origins of the new solution with respect to the periodic model. When the limit point, given by l_N in figure 6, was traced back to $\tau = 0$, it remained as a limit point. This is contrary to what we might have expected, since all the previously known solutions bifurcate in some continuous manner from the trivial solution. Figure 8 represents the projection of the set of these limit points onto the (Γ, R)-plane at $\tau = 0$, compared with the pitchfork bifurcation to five-cell flow in the existing model.

We computed the solution along both branches of the new five-cell flow, at $\tau = 0$, to a value of $R = 1000$. Both branches remain regular. An interesting point to note is that the solution on the stable branch mutates smoothly from the five-cell state to a three-cell state which is not connected to the previously recorded three-cell state. This unusual phenomenon does not occur at $\tau = 1$. A streamline plot of the stable, new five-cell solution, at $R = 90$, is shown in figure 9(*a*). As the Reynolds number is

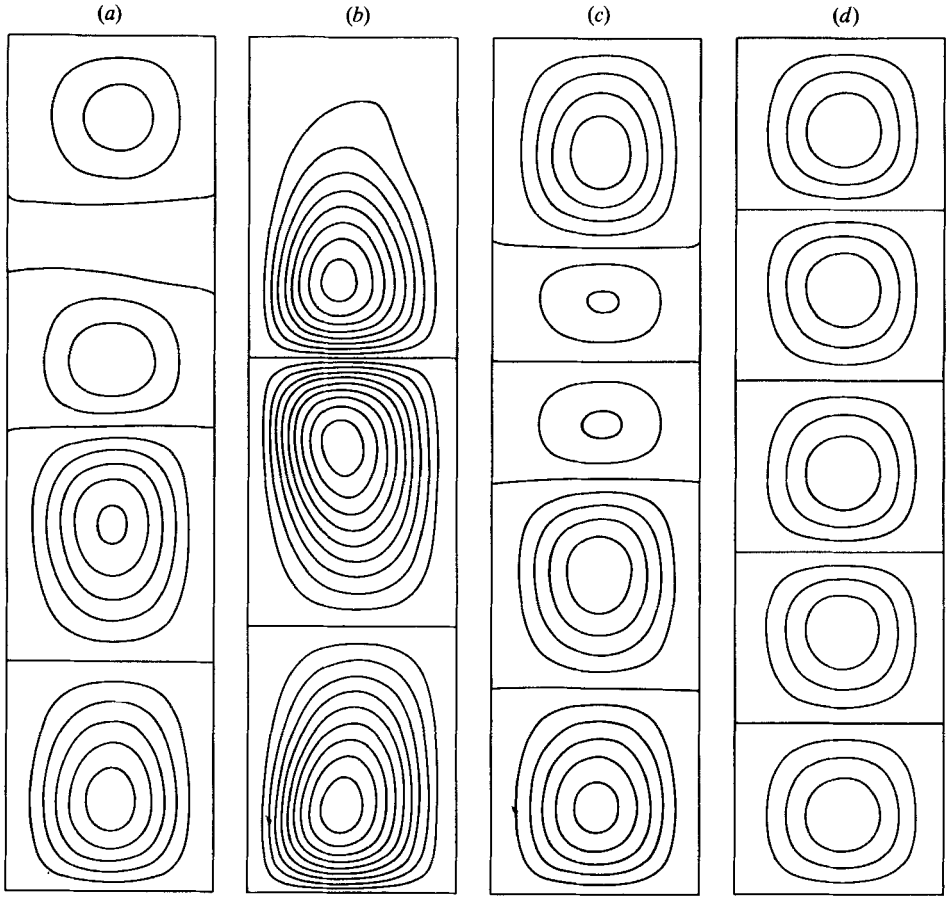

FIGURE 9. Streamline plots of the solutions at $\tau = 0$, $\Gamma = 4.0$. Contours of the streamfunction are plotted at intervals of 0.01. (*a*) Stable, new flow at $R = 90$; (*b*) stable, new flow at $R = 200$; (*c*) unstable, new flow at $R = 90$; (*d*) standard five-cell flow at $R = 90$.

increased the very weak cell collapses and the end cell is absorbed into the third cell up to produce a three-cell flow which is shown in figure 9(*b*). The unstable, new five-cell solution, at $R = 90$, is shown in figure 9(*c*) and, for comparison, the old five-cell solution, at $R = 90$, is shown in figure 9(*d*).

Finally, we find that there is no effect on the disconnected nature of the solution when the radius ratio is increased to 0.98. Therefore, we cannot attribute the new solution to the more complex nature of the wide-gap problem.

4. Conclusions

We have used the ideas of Schaeffer (1980) to compute the stability curve for the well-known anomalous five-cell flow solution of the realistic model. Numerical methods have been applied to compute a path of limit points using a continuation process. We find that there are three singularities on the path of limit points, namely a hysteresis point, a transcritical bifurcation point and a Takens–Bogdanov point. We deduce from these observations that another solution is interacting with the well-known solution. The 'new' solution has been computed numerically and the results show that it is another five-cell flow.

The new state has been observed experimentally, and comparisons between numerical and experimental results show that it is stable for aspect ratios below about 3.91. Over the same range of aspect ratios the well-known state, which we refer to as the 'old' solution, is not stable. However, for aspect ratios greater than 3.93 the old solution is stable and the new one is unstable. A comparison of the two states using cross-sectional photographs and streamline plots, shows that they are clearly different.

We use a bifurcation theory approach to explain the exchange in stability. In particular, a path of Hopf bifurcation points, which gives rise to unstable time-dependent flow, has an important effect on the stability of the steady-state solution.

The result is that we expect the steady-state solution to lose stability below different curves, depending on the value of aspect ratio. In fact there are three different regions. For Γ less than 3.91, where the new solution is stable, the flow loses stability at a limit point. For Γ in the range 3.91 to 4.14 the stable steady flow loses stability at a hopf bifurcation point. In this region we would expect to observe the old solution for Γ greater than 3.93, whilst for Γ less than 3.93 the nature of the solution is unclear. Finally, for Γ greater than 4.14 the old solution is stable and the flow loses stability at a limit point. The loss of stability of the experimentally observed steady-state flow compares favourable with the stability curves obtained numerically using continuation methods.

The new solution was studied numerically by following the path of limit points from $\tau = 1$ to $\tau = 0$. At $\tau = 0$ the new five-cell state is quite different to the old one. While the old solution bifurcates from the trivial Couette flow branch at a critical value of R, the new five-cell state is completely disconnected and loses stability at a limit point. We used continuation techniques to compute both branches of the solution up to a value of $R = 1000$ and found them to be regular. We, therefore, refer to this new five-cell state as a disconnected mode.

Finally, we computed the solution at values of radius ratio up to $\eta = 0.98$ to determine whether we were observing a phenomenon restricted to the wide-gap problem. This proved not to be the case and we conclude that the new solution is disconnected over all parameter space.

The research of D.K.A. was supported by an SERC CASE studentship with Harwell Laboratory, T.M. by the SERC Nonlinear Initiative and K.A.C. by the Underlying Programme of the UKAEA and by the Royal Society under the Royal Society/SERC Industrial Fellowship scheme.

REFERENCES

Benjamin, T. B. 1978 Bifurcation phenomena in steady flows of a viscous liquid. I. Theory. *Proc. R. Soc. Lond.* A **359**, 1–26.

Benjamin, T. B. 1978*b* Bifurcation phenomena in steady flows of a viscous liquid. II. Experiments. *Proc. R. Soc. Lond.* A **359**, 27–43.

Benjamin, T. B. & Mullin, T. 1981 Anomalous modes in the Taylor experiment. *Proc. R. Soc. Lond.* A **377**, 221–249.

Bolstad, J. H. & Keller, H. B. 1987 Computation of anomalous modes in the Taylor experiment. *J. Comput. Phys.* **69**, 230–251.

Cliffe, K. A. 1983 Numerical calculations of two-cell and single-cell Taylor flows *J. Fluid Mech.* **135**, 219–233.

Cliffe, K. A. & Mullin, T. 1985 A numerical and experimental study of anomalous modes in the Taylor experiment. *J. Fluid Mech.* **153**, 243–258.

CLIFFE, K. A. & SPENCE, A. 1984 The calclation of high order singularities in the finite Taylor problem. In *Numerical Methods for Bifurcation Problems* (ed. T. Küpper, H. D. Mittelman & H. Weber), pp. 129–144. ISNM, Birkhäuser.

GRIEWANK, A. & REDDIEN, G. 1983 The calculation of Hopf points by a direct method. *IMA J. Numer. Anal.* **3**, 295–303.

GUCKENHEIMER, J. & HOLMES, P. J. 1986 *Nonlinear Oscillations, Dynamical Systems, and Bifurcations of Vector Fields.* Springer.

JEPSON, A. D. & SPENCE, A. 1985 Folds in solutions of two parameter systems and their calculation Part I. *SIAM J. Numer. Anal.* **22**, 347–368.

JEPSON, A. D., SPENCE, A. & CLIFFE, K. A. 1988 Hopf along a fold. *Harwell Rep.* AERE-TP. 1264.

KELLER, H. B. 1977 Numerical solutions of bifurcation and nonlinear eigenvalue problems. In *Applications of Bifurcation Theory* (ed. P. H. Rabinowitz), pp. 359–384. Academic.

MOORE, G. & SPENCE, A. 1980 The calculation of turning points of nonlinear equations. *SIAM J. Numer. Anal.* **17**, 567–576.

PFISTER, G., SCHMIDT, H., CLIFFE, K. A. & MULLIN, T. 1988 Bifurcation phenomena in Taylor–Couette flow in a very short annulus. *J. Fluid Mech.* **191**, 1–18.

SCHAEFFER, D. G. 1980 Analysis of a model in the Taylor problem. *Math. Proc. Camb. Phil. Soc.* **87**, 307–337.

WERNER, B. & SPENCE, A. 1984 The computation of symmetry-breaking bifurcation points. *SIAM J. Numer. Anal.* **21**, 388–399.